International Journal of Engineering, Mathematical and Physical Sciences
ISSN: 2517-9934
Vol:10, No:10, 2016

# Mathematical Reconstruction of an Object Image Using X-Ray Interferometric Fourier Holography Method

M. K. Balyan

***Abstract*—**The main principles of X-ray Fourier interferometric holography method are discussed. The object image is reconstructed by the mathematical method of Fourier transformation. The three methods are presented – *method of approximation, iteration method and step by step method*. As an example the complex amplitude transmission coefficient reconstruction of a beryllium wire is considered. The results reconstructed by three presented methods are compared. The best results are obtained by means of *step by step method.*

***Keywords*—**Dynamical diffraction, hologram, object image, X-ray holography.

## I. Introduction

THE existing methods of optical holography- the Fresnel holography,- the methods of on axis (Gabor) holography and off-axis holography, the Fraunhofer holography, the Fourier holography, the interferometric holography [1]-[3], may be elaborated in X-ray range of frequencies. X-ray holograms may be obtained based on the X-ray diffraction (Bragg) optics [4]. The method of X-ray interferometric holography was proposed in [5] and developed in [6], [7]. In this method, an object under investigation is placed in one of the interferometer arms, and the wave passing via the other arm of the interferometer is the reference wave. A method for reconstruction of a point source of X-ray waves was proposed in [8]. Using the synchrotron sources of X-ray waves, the methods of X-ray holography are developed: on-axis (Gabor) holography [9]-[12] and the Fourier holography [12]-[14].

The dynamical two-wave Laue diffraction on two slits is a simple dynamical diffraction Fourier holography method [15]. The Momose method is an X-ray interferometric phase contrast method, where the Fourier transform method is applied [16]. In [17]-[19], the Fraunhofer dynamical diffraction holography method, and in [20], the Fourier dynamical diffraction methods are proposed and theoretically investigated. The X-ray interferometric Fresnel holography is considered in [21] and the X-ray interferometric Fourier holography method in [22]. In this paper, we describe the X-ray Fourier interferometric method of holography, we present the three methods of reconstruction, and we compare the obtained results of the reconstructed amplitude transmission coefficient of a beryllium wire.

M. K. Balyan is with the Yerevan State University, Armenia, Yerevan 0025, AlexManoogian 1 (e-mail: mbalyan@ ysu.am).

## II. X-Ray Interferometric Fourier Holography

Let us briefly consider the X-ray interferometric Fourier holographic scheme [22] and the basic formulas. Under the exact Bragg angle an X-ray monochromatic plane wave with unit amplitude falls on the three block X-ray interferometer (Fig. 1).

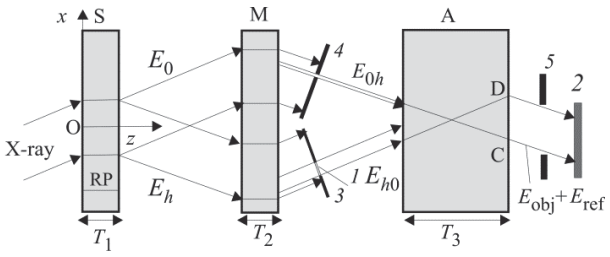


Fig. 1 X-ray interferometric Fourier holography scheme. S, M, A are splitter, mirror and analyzer blocks, RP- the reflecting planes, Oxz the coordinate system, CD the rang where the hologram is recorded, 1- object, 2- hologram, 3,4,5- slits, $E_0$, $E_h$, $E_{0h}$, $E_{h0}$, $E_{obj}+E_{ref}$ - the amplitudes of beams in the interferometer

In one of the arms of the interferometer, an object with amplitude transmission coefficient $t(x,y)$ is placed. The amplitude $E_{hol}$ may be presented in the form

$$E_{hol} = E_{ref} + E_{obj} \tag{1}$$

where $E_{ref}$, $E_{obj}$ are the amplitudes of the reference and object waves, respectively. According to (1), the intensity distribution on the exit surface of the analyzer (the third plate of the interferometer) will be

$$I_{hol} = \left|E_{ref}\right|^2 + E_{ref}E_{obj}^* + E_{ref}^*E_{obj} + \left|E_{obj}\right|^2 \tag{2}$$

We consider the case when $T_3/\Lambda_r >> 1$ and $\mu T_3 >> 1$, where $T_3$ - the thickness of the analyzer, $\mu$ - linear absorption coefficient of the interferometer blocks, $\Lambda_r$ – the extinction length. The two first plates of the interferometer may have lesser thicknesses, but so, that $T_1 = T_2 < T_3$ and $\mu T_{1,2} > 1$. In this case, only the weakly absorbing mode of σ-polarization may be taken into account [23], [24]. According to the dynamical theory of X-ray diffraction [23]-[25], the amplitudes may be presented in the form

$$E_{\text{obj}} = \frac{1}{4}\exp(2i\sigma_0 T_1)\int_{x_{\text{obj}1}}^{x_{\text{obj}2}} G_{h0}(x-x',T_3)t(x',y)dx', \quad (3)$$

$$E_{\text{ref}} = -\frac{1}{4}\exp(2i\sigma_0 T_1)\int_{x_{\text{ref}1}}^{x_{\text{ref}2}} G_{hh}(x-x',T_3)dx' \quad (4)$$

where $x_{\text{ref1,2;obj1,2}}$ are the coordinates of the reference and object waves left and right bounds on the exit surface of the analyzer, $\sigma_0 = k\chi_0/(2\cos\theta) + \pi/\Lambda$, $k = 2\pi/\lambda$ - the wave number, $\chi_0 = \chi_{0r} + i\chi_{0i}$ – the zero-order Fourier component of the crystal susceptibility, $\Lambda = \lambda\cos\theta/(\chi_h\chi_{-h})^{1/2}$ ($\Lambda_r = \text{Re}\Lambda$ is the extinction length), $\chi_h = \chi_{-h} = \chi_{hr} + i\chi_{hi}$ – the Fourier coefficients of the crystal susceptibility corresponding to the diffraction vectors **h** and –**h** (without loss of the generality we consider the case of a centrally-symmetrical crystal), θ - the Bragg angle. The expressions of the Green functions $G_{h0}$ and $G_{hh}$ are given in [24], [25]. Used here the Green functions are obtained presented in [25] multiplying them by $\exp(ik\chi_0 T_3/2\cos\theta)$. The slit of the reference wave is narrow and in (4) one may take the Green function out of the integral sign

$$E_{\text{ref}} = -\exp(2i\sigma_0 T_1)(2a_{\text{ref}})G_{hh}(x-x_{\text{ref}},T_3)/4 \quad (5)$$

where $x_{\text{ref}}$ is the coordinate of the reference wave center and $2a_{\text{ref}}$ – the size of the projection of the reference wave slit on the entrance surface of the analyzer. In [22], it has been shown, that the object wave amplitude (3) is proportional to the Fourier transform of the object amplitude transmission coefficient. Therefore, for reconstruction of the amplitude transmission coefficient, the intensity distribution (2) must be multiplied by $\exp(-2\pi ipx/D_1)$ and integrated over the hologram surface

$$E_{\text{rec}} = \int_{-\infty}^{+\infty} \exp(-2\pi ipx/D_1)I_h(x,y)dx \quad (6)$$

where $D_1 = T_3\Lambda_r\text{tg}^2\theta/x_{\text{ref}}$, is a parameter. According to (2), (6) is a sum of four terms. For the second and the third terms in [22], the following approximate expressions are found

$$E_{\text{rec}2} = 2(2a_{\text{ref}})|Q|^2 Dt^*(x_{\text{ref}} - 2px_{\text{ref}}, y) \quad (7)$$

$$E_{\text{rec}3} = 2(2a_{\text{ref}})|Q|^2 Dt(x_{\text{ref}} + 2px_{\text{ref}}, y) \quad (8)$$

According to these expressions, (7) is the conjugate reconstructed image, and (8) is the direct real image of the object. The conjugate image is concentrated near the $p = 1$ and for the conjugate image $1-a_{\text{obj}}/2x_{\text{ref}} \le p \le 1+a_{\text{obj}}/2x_{\text{ref}}$, meanwhile the image is rotated by $180^\circ$. The real image (8) is concentrated around $p = -1$ and $-1-a_{\text{obj}}/2x_{\text{ref}} \le p \le -1+a_{\text{obj}}/2x_{\text{ref}}$. Taking the values of $I_{\text{hol}}$ from the experiment and calculating the integral (6) from (8) one may find the approximate values of the amplitude transmission coefficient of the object under investigation. This is the analytical, *approximate method* of reconstruction. According to the *analytical approximation* (6)-(8) the zero order approximation will be

$$t(x,y) = t_0(x,y) = E_{\text{rec}}(p)/E_{\text{rec3,s}}(p) \quad (9)$$

where $E_{\text{rec3,s}}(p)$ is obtained from the expression of $E_{\text{rec3}}(p)$ and there $t(x,y) = 1$. The relation between $p$ and $x$ is given by $p = x/(2x_{\text{ref}}) - 1/2$ and $x$ is in the interval $-x_{\text{ref}} - a_{\text{obj}} \le x \le -x_{\text{ref}} + a_{\text{obj}}$. The corresponding $p$ lies in the interval $-1 - a_{\text{obj}}/(2x_{\text{ref}}) \le p \le -1 + a_{\text{obj}}/(2x_{\text{ref}})$. *The next approximation* is obtained [22] when for calculating $E_{\text{rec3}}(p)$ to expand $t(x', y)$ near the point $x'_0 = 2px_{\text{ref}} + x_{\text{ref}}$ into Taylor series taking into account the linear terms and for the value at $x'_0$ to use (9). By this way we obtain

$$t(x,y) = t_1(x,y) = t_0(x,y) - E^{(1)}{}_{\text{rec3}}(p)/E_{\text{rec3,s}}(p) \quad (10)$$

where $E^{(1)}{}_{\text{rec3}}(p)$ is obtained from the expression $E_{\text{rec3}}(p)$ substituting $t(x,y)$ by $t_0'(x_0',y)(x' - x'_0)$, $t_0'(x_0',y)$ is the derivative of $t_0(x,y)$ at the point $x_0' = 2px_{\text{ref}} + x_{\text{ref}}$. The *iteration procedure* may be continued.

Instead of the iteration procedure a *step by step* method may be used [22]. In this method, one takes the object narrow slit (Fig. 1). Suppose that the object slit has the same width as the reference wave's slit. The right (or left) edge of the object is set on the left (right) edge of the object slit. After moving the object by a step (equal or not equal to the object slit size), the Fourier hologram of this section of the object is recorded. This procedure is repeated by $N = a_{\text{obj}}/a_{\text{ref}}$ times, and at each step, the Fourier hologram of the corresponding section of the object is recorded. After all displacements of the object, we obtain $N$ holograms for the whole $2a_{\text{ref}}$ size of the object. If the object slit is sufficiently narrow, one may assume that $t_i(x, y)$ ($i = 1\ldots N$) is a constant and is determined by the expression

$$t_i(-x_{\text{ref}}, y) = E_{\text{rec}i}(-1)/E_{\text{rec3i,s}}(-1) \quad (11)$$

where $E_{\text{rec}i}(-1)$ and $E_{\text{rec3i,s}}(-1)$ have the same sense as in (9) but for the step $i$. So, the object amplitude transmission coefficient is constructed by means of $N$ values of $t_i(-x_{\text{ref}}, y)$ ($i = 1\ldots N$), by obtaining $N$ holograms for $p = -1$. The interpolation of the obtained function given by these $N$ values complete the problem of finding $t(x,y)$.

## III. An Example and Comparison of the Results of Various Methods

Let us consider an example of object amplitude transmission coefficient $t(x, y)$ reconstruction for a beryllium

wire by the radius $R_{ob} = 50\,\mu m$ and with the axes perpendicular to the diffraction plane. The width of the object slit is equal to $2R_{ob}$, and the width of the reference wave slit is equal to 4 μm, $x_{ref} = 50/\cos\theta$ μm, $x_{obj} = -x_{ref}$. We consider the reflection $Si(220)$, $\lambda = 0.71\,\mathring{A}$ (17.46 keV), $T_1 = T_2 = 1\,mm$, $T_3 = 5\,mm$. The refractive index of the object is $n = 1 - \delta + i\beta$, $\delta > 0$ and is connected with the refraction in the object, $\beta > 0$ and is connected with the absorption in the object. For beryllium $\delta = 1.118 \cdot 10^{-6}, \beta = 2.69 \cdot 10^{-10}$. The theoretical expression for $t(x, y)$ is

$$t(x, y) = \exp[-2ik(\delta - i\beta)\sqrt{R_{ob}^2 - (x + x_{ref})^2 \cos^2\theta}]. \quad (12)$$

Let us calculate $I_{hol}$ using (2) and (12) and let us assume that these calculated values are experimentally obtained values of the intensity of the object Fourier hologram. Then using (9), one obtains zero order approximation - $t_0(x, y)$. In Fig. 2, the intensity distribution (2) on the hologram is presented.

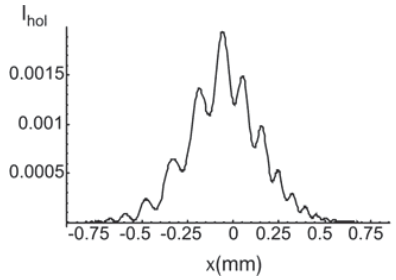


Fig. 2 The intensity distribution on the Fourier interferometric hologram of the beryllium wire

In Figs. 3 (a) and (b), the real and imaginary parts of the object amplitude transmission coefficient $t_0(x)$ obtained by means of the *zero order approximation* (9) are presented and are compared with the corresponding true values $t(x)$ (12). The resolution is sufficient to reconstruct the amplitude transmission coefficient in the middle part of the wire, but it is not sufficient at the edges of the wire.

In Figs. 4 (a) and (b), the real and imaginary parts of the object amplitude transmission coefficient are presented using the *first order iteration* (10). These values are compared with the corresponding true values of $t(x)$ (12).

As it is seen from Figs. 3 and 4, the first iteration gives more precise results than the approximation of the zero order.

Instead of continuing the iterations, let us determine the amplitude transmission coefficient of the beryllium wire using the described above *step by step* method of reconstruction.

Let us take the width of the object wave the same as for the reference wave, i.e. 4 μm, the step of the displacement 4μm, $x_{ref} = 25/\cos\theta$ μm, $x_{obj} = -x_{ref}$. For $N = 25$, let us calculate all $I_{holi}(x)$ ($i$=1,…,25) and let us determine $t_i$ using (11). Let us construct the interpolation function using these 25 values. In Fig. 5, the hologram for the step $i$=13 is shown (for this step the center of the object is coincided with the center of the object slit). In Figs. 6 (a) and (b), real and imaginary parts of the object amplitude transmission coefficient obtained by the *step by step* method are compared with the corresponding true values (12). It is clearly seen that the more precise results are obtained by the *step by step* method in comparison with the approximation and iteration methods. The obtained values are almost the same as the true values.

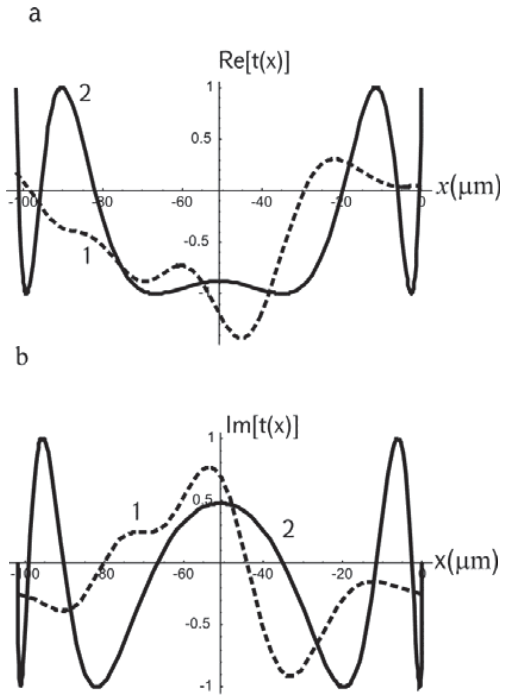


Fig. 3 The comparison of the zero order reconstructed real and imaginary parts of the beryllium wire amplitude transmission coefficient with the corresponding true values (12). a. 1- the reconstructed zero order approximation value of the real part $t_0(x)$ (dashed line), 2- the real part of the true value (solid line); b. 1-the reconstructed zero order approximation value of the imaginary part $t_0(x)$ (dashed line), 2- the imaginary part of the true value (solid line)

## IV. Conclusions

The main principles of the X-ray Fourier interferometric holographic method are presented and discussed. The reconstruction of the object amplitude transmission coefficient is obtained by means of three methods – *approximation method*, *iteration method* and *step by step* method. As an example, the reconstruction of the beryllium cylindrical wire amplitude transmission coefficient is considered. The results of three methods of reconstruction are compared with each other and with the true values of the amplitude transmission coefficient. The best results are obtained by the *step by step method* of reconstruction.

The method of the X-ray interferometric Fourier holography may be experimentally realized with the help of X-ray synchrotron sources and XFELs. The method may be used in X-ray microscopy for determination amplitude transmission coefficient of inhomogeneous objects (the amplitude and the phase ones) as well as for determination of the density of objects (of its internal structure) and of the refractive index.

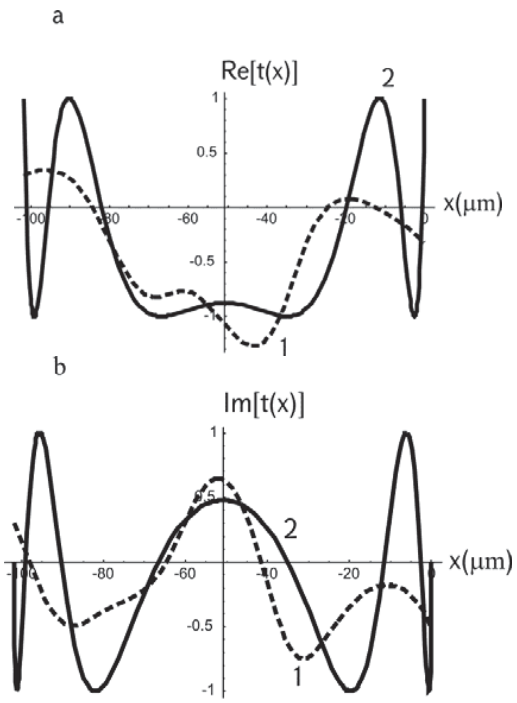


Fig. 4 The comparison obtained by (10) by the first order iteration of the real and imaginary parts of the beryllium wire amplitude transmission coefficient with the corresponding true values (12). a. 1- the reconstructed value of the real part $t_1(x)$ (dashed line), 2- the real part of the true value (solid line); b. 1-the reconstructed value of the imaginary part $t_1(x)$ (dashed line), 2- the imaginary part of the true value (solid line)

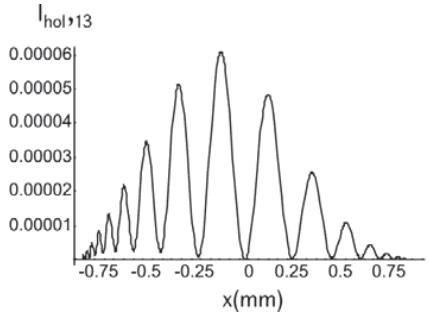


Fig. 5 The intensity distribution on the X-ray Fourier interferometric hologram of the wire obtained by means of step by step method for the step $i$=13

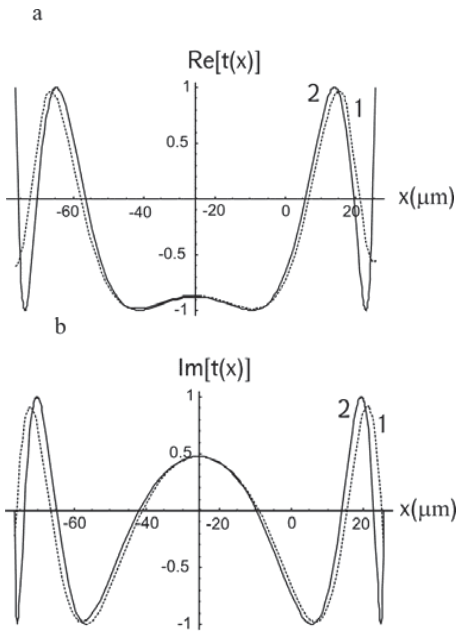


Fig. 6 The comparison obtained by (11) of the *step by step method* of the real and imaginary parts of the beryllium wire amplitude transmission coefficient with the corresponding true values (12). a. 1- the reconstructed value of the real part (dashed line), 2- the real part of the true value (solid line); b. 1-the reconstructed value of the imaginary part (dashed line), 2- the imaginary part of the true value (solid line)

## References

[1] R. G. Collier, Ch. B. Burckhardt, L. H. Lin, "Optical holography", New York and London, Academic Press, 1971.
[2] P. Hariharan, "Basics of holography", New York, Cambridge University Press, 2002.
[3] "Handbook of optical holography", H. J. Caulfield, Ed., Bedford, Massachusets, Aerodyne research Inc., 1979.
[4] V. V. Aristov, G. V. Ivanova, "On the possibility of utilizing holographyc schemes in X-ray microscopy", J. Appl. Cryst., v. 12, pp. 19-24, Febr. 1979.
[5] A. M. Egiazaryan and P. A. Bezirganyan, "The recording of X-ray short-wave hologram", Proc. Nat. Acad. Sci. Armen. Phys., v. 15, pp.35-43, 1980 (in Russian).
[6] A. M. Egiazaryan, "The new perspectives of development of X-ray short-wave holography", JTP, Pisma, v.24, pp.55-59, 1998 (in Russian).
[7] A. M. Egiazaryan, K. G. Trouni and A. R. Mkrtchyan, "X-ray interferometric short-wavelength holography with diffraction focusing", JETP Letters, v.68, pp.711-715, 1998.
[8] K. T. Gabrielyan, "Using of crystal-diffraction image for obtaining visible image of an X-ray source", JTP, Pisma, v.16, pp.5-9, 1990 (In Russian).
[9] A. Snigirev, I. Snigireva, V. Kohn, S. Kuznetsov and I. Schelokov, "On the possibilities of X-ray phase-contrast microimaging by coherent high-energy synchrotron radiation", Rev. Sci. Instrum., v.66, pp.5486-5492, 1995.
[10] K. A. Nugent, T. E. Gureyev, D. F. Cookson, D. Paganin and Z. Barnea, "Quantitative phase imaging using hard X-rays", Phys. Rev. Lett., v.77, pp.2961-2964, 1996.
[11] D. M. Paganin, "Coherent X-ray Optics", Oxford, Oxford University Press, 2006.
[12] N. Watanabe, H. Yokosuka, T. Ohogashi, H. Takano, A. Takeuchi, Y. Suzuki and S. Aoki, "Optical holography in the hard X-ray domain", J. Phys IV France, v.104, pp. 551-556, 2003.
[13] W. Leitenberger and A. Snigirev, "Microscopic imaging with high energy X-rays by Fourier transform holography", J. Appl.Phys., v.90, pp. 538-544, 2001.

[14] H. Iwamoto and N. Yagi, “Hard X-ray Fourier transform holography from an array of oriented referenced objects”, J. Synchrotron Rad., v.18, pp. 564-568, 2011.
[15] M.K. Balyan, “Double slit dynamical diffraction of X-rays in ideal crystals (Laue case)”, Acta Cryst., v. A66, pp. 660-668, 2010.
[16] A. Momose, “Demonstration of phase contrast X-ray computed tomography using an X-ray interferometer”, Nucl. Instr. Meth., v.A352, pp. 622-628, 1995.
[17] M. K. Balyan, “X-ray dynamical diffraction Fraunhofer holography”, J. Synchrotron Rad., v.20, pp. 749-755, 2013.
[18] M. K. Balyan, “Numerical reconstruction of an object image using an X-ray dynamical diffraction Fraunhofer hologram”, J. Synchrotron Rad., v.21, pp. 127-130 (2014).
[19] M. K. Balyan, “Object image correction using an X-ray dynamical diffraction Fraunhofer hologram”, J. Synchrotron Rad., v.21, pp. 449-451, 2014.
[20] M. K. Balyan, “X-ray crystal-diffraction Fourier holography”, J. Contemp. Phys. Arm. Acad. Sci., v.50, pp.394-403, 2015.
[21] M. K. Balyan, “X-ray interferometric Fresnel holography”, J. Contemp. Phys. Arm. Acad. Sci., v.51, pp.79-88, 2016.
[22] M. K. Balyan, “X-ray interferometric Fourier holography”, Proceed. of Natl. Acad. Sci. Arm., v.51, pp.388-401, 2016 (In Russian).
[23] A. Authier, “Dynamical Theory of X-ray Diffraction”, Oxford, Oxford University Press, 2001.
[24] Z. G. Pinsker, “X-ray crystalloptics”, Moscow, Nauka, 1982 (In Russian).
[25] V. L. Indenbom, F. N. Chukhovskii, "The problem of image formation in X-RAY optics", Sov. Phys. Usp., v.15, pp.298–317, 1972.